Journal of the European Ceramic Society **15** (1995) 283–289

0955-2219/95/$9.50

Microstructure and Mechanical Properties of Textured Al_2O_3

T. Carisey, I. Levin & D. G. Brandon

Department of Materials Engineering, Technion — Israel Institute of Technology, Haifa 32000, Israel

(Received 19 April 1994; revised version received 5 July 1994; accepted 2 August 1994)

Abstract

The mechanical properties of a highly textured alumina have been studied and show a significant improvement in bend strength and Weibull modulus when compared to a randomly textured alumina of similar purity. The crystalline texture was due to growth of a small concentration of aligned and uniformly distributed alumina seed platelets into a fine-grained powder matrix during sintering. The (0001) texture of the sintered product gave a non-equiaxed, flattened grain structure, with the c*-axis of the hexagonal unit cell approximately normal to the plane of the specimen tiles. This highly textured microstructure drastically reduces the residual stresses which are associated with thermal contraction anisotropy in polycrystalline alumina, and inhibits crack propagation in the through-thickness direction. Two platelet sizes were investigated, the smaller of which gave the smaller final grain size and the better mechanical properties. At 5 wt% of platelet additions the properties were significantly more reproducible than at 10 wt% of the platelets, probably because of significant interference in packing the platelets at the higher loading.*

Introduction

The main limitation on the use of ceramics as structural materials is their brittleness. The production of a microstructurally and crystallographically oriented monolithic ceramic could be one route towards improving the strength and the resistance to crack propagation, since an oriented and textured monolithic ceramic should avoid some of the problems associated with reinforcement by a second phase; in particular, mismatch of the chemical, thermal or elastic properties of the reinforcing and matrix phases.

Previous work[1] on an alumina matrix reinforced with SiC whiskers has shown that the bend strength and the fracture toughness can be improved, although the whiskers need to be handled with care because of the health problems associated with possible ingestion. SiC platelet reinforcement is also effective, and reinforcement of a ceramic matrix with aligned SiC platelets has been shown to give mechanical anisotropy. For example,[2] the addition of 30% of SiC platelets to a Si_3N_4 matrix powder increased the fracture toughness, the Weibull modulus and Young's modulus of the hot-pressed product, while the mechanical anisotropy was demonstrated in indented samples, for which the extent of crack propagation parallel and perpendicular to the direction of hot- pressing was markedly different.

The bend strength of a zirconia matrix[3] with 5% of SiC platelet additions was reported to be slightly improved from room temperature to 600°C, while the toughness of the composite was about 50% higher than the matrix. The same matrix when reinforced with alumina platelets[4] gave a high toughness and bend strength with 10% of platelet additions from room temperature up to 800°C, and at 1400°C high strain rates resulted in 17% plastic deformation over 30 min, suggesting the onset of super plastic behaviour.

The effect of the shape of the reinforcement has been considered in other work on crack propagation[5,6] and whiskers and platelets were compared. The crack path was found to depend on the shape, size and volume fraction of the second phase particles. These were precipitated by heat treatment in a lithium-alumino-silicate glass ceramic. The fracture toughness was found to be invariant with the particle size.

The present work reports the mechanical properties of a crystallographically textured monolithic alumina produced by gel-casting of a slip containing aligned seed platelets.[7] The bend strength, Weibull modulus, fracture toughness and hardness are compared and correlated with the crystalline texture, the microstructural anisotropy and grain-size, and the state of internal stress. Vickers indentation cracking has been used to demonstrate the anisotropy of the crack propagation resistance.

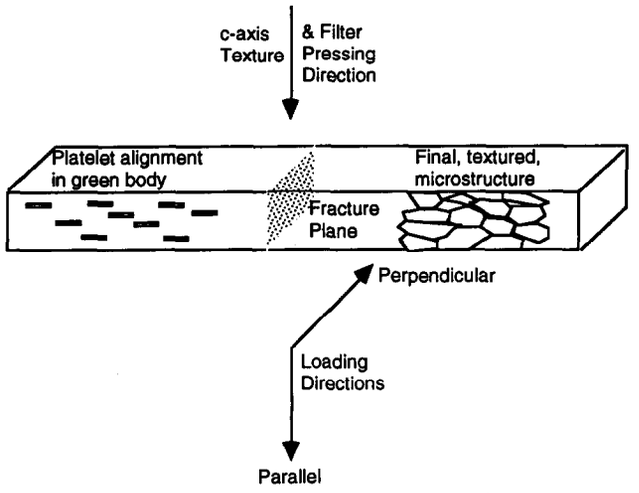

Fig. 1. Seed platelet and bend-bar geometries for textured alumina specimens.

Experimental

Composite fabrication

Highly textured monolithic alumina plate samples were prepared with the *c*-axis of the hexagonal unit cell within 10° of the normal to the plate surface. The samples were prepared by filter compaction and sintering of wet, water-based, gelled tape containing alumina seed platelets which had been aligned by a doctor-blade gel-casting process, as described previously.[7] The textured aluminas were compared with untextured (randomly oriented) samples prepared from the same powder and using the same processing route (water-based tape-casting, followed by lay-up, filter pressing and pressureless sintering), but with no seed platelet additions.

Characterization

Optical and scanning electron microscopy (SEM) were used to characterize the microstructure of polished cross-sections of the pressureless-sintered tile samples. Crack propagation was studied by varying the orientation of a Vickers indentation on polished sections cut perpendicular to the plate surface. SEM was the preferred method for evaluating the sintered microstructure, the fracture surfaces of bend specimens and the indentation crack morphology. The indentation samples were polished but unetched, while all other sintered specimen sections were polished and thermally etched at 1450°C for 30 min.

Mechanical testing

The sintered tiles were sectioned into 30 × 4 × 3 mm test bars with a 20 mm load span. The bend strength[8] was determined in 3-point bending for samples in which the tensile surface was either parallel or perpendicular to the plane defined by the original, aligned seed platelets. That is, the plane of the fracture was always the same, but the normal to the tensile surface was either parallel or perpendicular to the principal *c*-axis of the textured samples (Fig.1). The specimen span was 20 mm. About 25 samples were tested to allow for Weibull analysis of the strength data.[9,10] The fracture toughness was measured using the single edged notched beam test (SENB)[11,12] and was determined for the same fracture plane and failure directions as in the bend tests. The hardness was determined by Vickers indentation at 50 N with the loading axis either parallel or perpendicular to the normal to the original platelets (the principal *c*-axis of the textured samples), taking the average of measurements made on 10 separate indentations.

Thermal stresses

The thermal stresses present in the sintered tiles were evaluated by X-ray diffraction peak-shift measurements, as described elsewhere.[13] These measurements were taken from polished surface sections cut parallel and perpendicular to the original plane of alignment of the seed platelets. The accuracy of the measurements was limited to approximately 1 part in 10^5 by the X-ray goniometer and the positioning of the sample. The reflections used were a compromise between the requirements for reasonable signal intensity and the need to sample strains parallel and perpendicular to the *c*-axis of the textured alumina grains. The reflections chosen were 41·6 and 41·0, for which the penetration depth at 90% absorption of the incident X-ray beam is about 80 μm, much larger than the observed grain size of the samples. The average microstrain perpendicular to the sample surface for the crystallographic directions corresponding to the planes satisfying the reflecting conditions is obtained from the reflection shift with respect to a standard powder sample. For the sample section cut perpendicular to the alignment plane, the measured strains are predominantly from the textured grains, while it is the residual, randomly-oriented grains which dominates the strain measurement from the parallel section. The prediction is that thermal stresses should be absent if the material contains only ideally textured grains with the *c*-axes fully aligned, since α-Al_2O_3 has only two coefficients of thermal expansion, parallel and perpendicular to the *c*-axis, the former exceeding the latter by about 10% at all temperatures.

Results

Figures 2 (a) and (b) show the bend strengths for two seed-platelet concentrations (5 and 10 wt%)

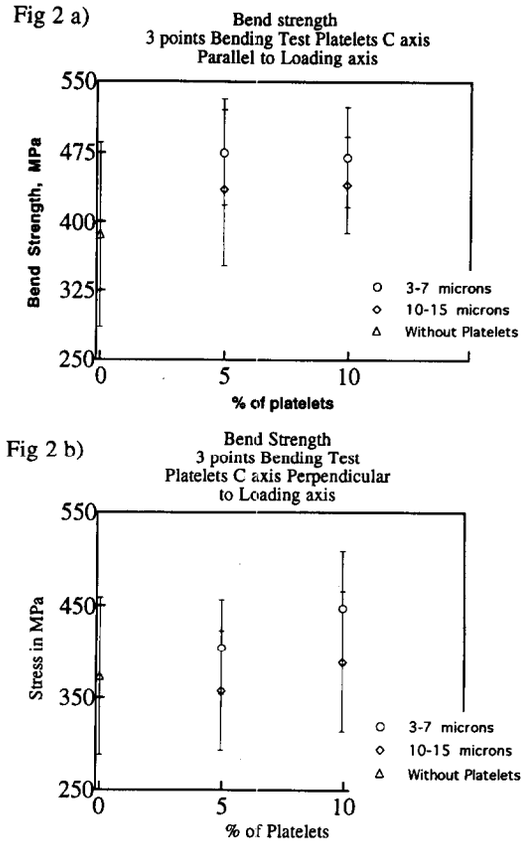

Fig. 2. Bend strength vs platelet concentration for both sizes of seed platelet additions: (a) principal *c*-axis of the textured tile parallel to the loading axis, (b) principal *c*-axis of the textured tile perpendicular to the loading axis.

and sizes (3–7 and 10–15 μm). The scatter bands shown are those calculated separately for each set of test results. In Fig. 2 (a) the tensile surface is parallel to the plane of the platelets, while in Fig. 2 (b) the plane of the tensile surface is perpendicular to the plane of the platelets. Clearly, the texture increases the bend strength when the tensile surface is parallel to the plane of the platelets, even though the grain size of the platelet-seeded and textured material is far larger than that of the unseeded alumina. The increase in bend strength after seeding with the smaller and larger platelets is 25 and 15%, respectively. In all cases the smaller seed platelets gave the smaller final grain size and were more effective than the larger ones in strengthening the product. The bend strength for crack propagation parallel to the principal *c*-axis of the texture was higher than that perpendicular to this axis. The mechanical behaviour of the specimens seeded with the larger platelets and with the tensile surface perpendicular to the original plane of the platelets was similar to that of alumina sintered without seed platelets, in spite of the much larger grain size of the seeded material, but with both sizes of seed platelets, the bend strength increased with platelet loading.

Figure 3 shows the Weibull moduli determined on 25 samples for the case of the tensile surface

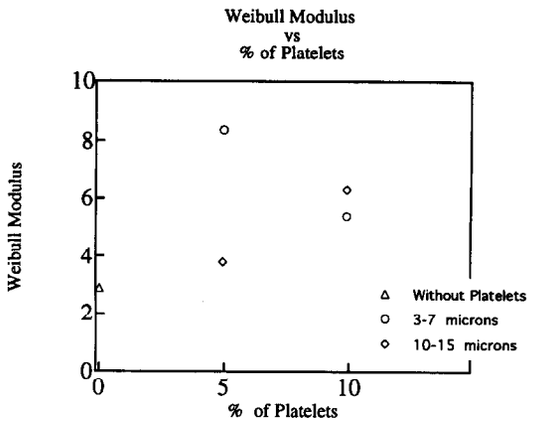

Fig. 3. Weibull modulus vs platelet concentration: principal *c*-axis of the texture parallel to the loading axis.

parallel to the original platelets. In view of the small number of samples, these values lack significance, but the small scale of the laboratory units constructed for gel-casting, tape lay-up and filter-pressing is thought to be primarily responsible for the very low value observed for the samples with no seed platelets. The improvement in Weibull modulus with the addition of seed platelets is thought to be significant. The best value of the modulus (about 8) was obtained for 5% additions of the smaller platelets. The platelet seeding appears to have improved the reliability of the sintered product, in addition to the improvement in the average mechanical strength.

The results for fracture toughness are presented in Fig.4 which again shows the two cases of the tensile surface either parallel (Fig. 4(a)) or perpendicular (Fig. 4(b)) to the platelets. The average fracture toughness calculated for the sample without platelets is questionably high for alumina, but the large standard deviation for this material puts it within the range of the other, textured samples. In Fig 4(a), the smaller seed platelets gave a better fracture toughness than the larger platelets, while in Fig. 4(b) all the values are very close together. In effect, the fracture toughness of the textured alumina is about 5 MPa $m^{-1/2}$, almost independent of the parameters examined.

Figure 5 shows the Vickers hardness results; firstly, in Fig. 5(a), as a function of the loading of the two sizes of seed platelets and, secondly, Fig. 5(b), in a comparison of the hardness measured on a cross-section of the tile (loading axis perpendicular to the principal *c*-axis of the texture) with that on the tile surface (the surface parallel to the plane of alignment of the seed platelets). The indent shape and crack propagation on the tile surface were similar for both the textured and the randomly oriented alumina. The indent shape on the cross-section will be discussed further below, but the measured hardness on this cross-section

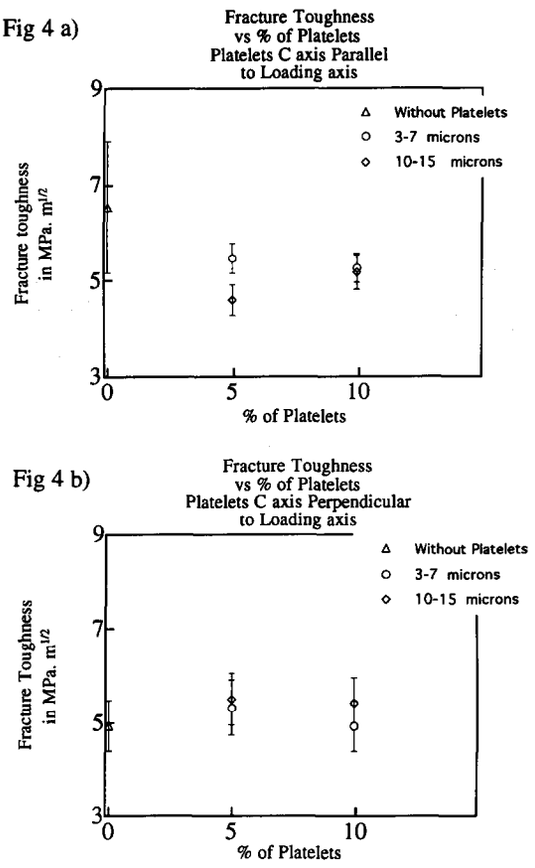

Fig. 4. Fracture toughness vs platelet concentration for both seed platelet sizes: (a) principal c-axis of the textured tile parallel to the loading axis; (b) principal c-axis of the textured tile perpendicular to the loading axis.

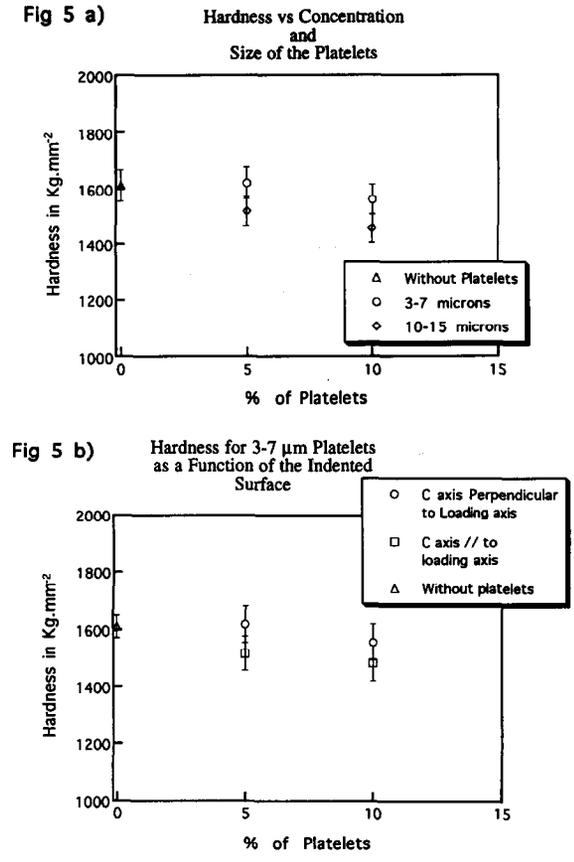

Fig. 5. Vickers hardness at 50 N vs platelet concentration: (a) for both sizes of seed platelet; (b) for two different indented surfaces: the sample cross-section and the surface parallel to plane of the original seed platelets.

was lowest for the smaller platelets (largest grain size), while the highest hardness, obtained for the sample without platelets, is associated with the small sintered grain size in the absence of the seed platelets.

The microstructure of the gel-cast alumina without platelets consisted of equiaxed grains with a grain size of about 3 μm. By contrast, the average grain size of the samples containing seed platelets was about 6 μm. The micrographs shown in Fig. 6 are taken from a tile cross-section. The non-equiaxed (oblate) grain structure is a result of the non-equiaxed distribution of the centres of gravity of the original aligned seed platelets. These have grown during sintering to consume most of the initial powder matrix. The final microstructure is highly textured and anisotropic, with a comparatively large grain size. It is the size of the original seed platelets and their volume fraction which determine the final grain size. A homogeneous distribution of the platelets[7] should give isotropic behaviour in the plane of the sample plate. In addition, grain growth has been enhanced by the presence of calcium in the green body associated with the current gel-casting process.

The mechanical anisotropy is demonstrated in Fig. 7, which shows optical micrographs of indented polished sections cut perpendicular to the tile surface. Figure 7(a) is from an indented sintered sample which contained no platelets, while Figure 7(b) shows a textured sample which contained 5 wt% of the smaller, aligned seed platelets. In the first case the cracks have the same length, while in the second case crack propagation parallel to the principal c-axis of the texture is clearly inhibited. Figure 8 shows SEM micrographs of indentation cracks, (a) propagating approximately parallel to the original direction of platelet alignment and (b) propagating approximately perpendicular to the alignment direction. In the first case, delamination has tended to generate a stepped surface, while in the second case the flattened, textured grains have inhibited crack propagation and given rise to a highly irregular crack path.

The thermal expansion coefficient α of alumina parallel to the c-axis is approximately 10% higher than that perpendicular to the c-axis, and is expected to lead to cumulative thermal strains in a random polycrystal cooled below the relaxation temperature. The total elastic mismatch at room temperature, $\Delta\alpha\Delta T$, assuming that the minimum value of ΔT is 1000°C, is about $7{\cdot}6 \times 10^{-4}$ in a random polycrystal. Assuming elastic isotropy, this will lead to a maximum c-axis compressive

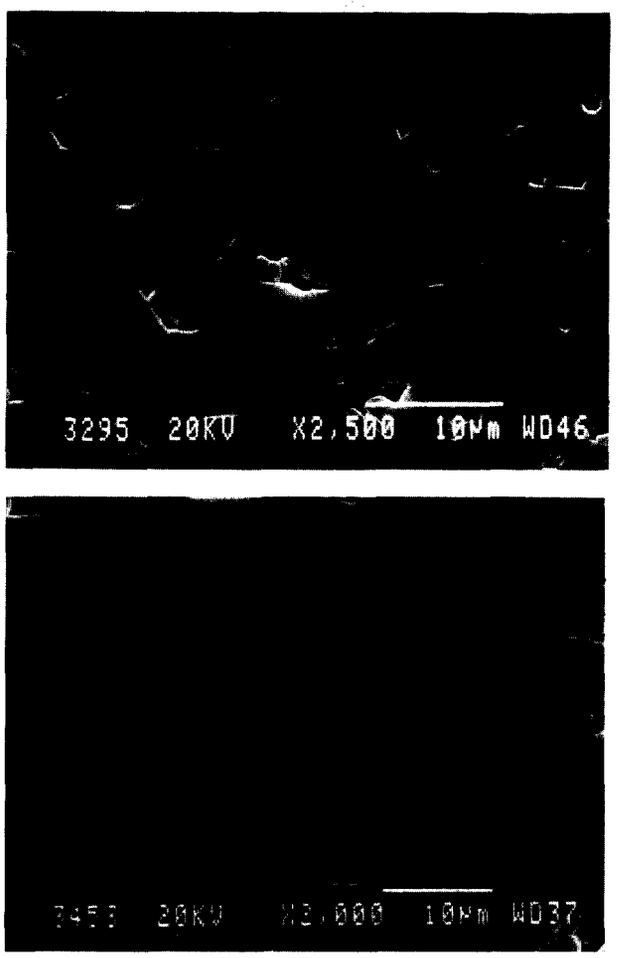

Fig. 6. SEM micrograph of thermally-etched samples: (a) sample with 5 wt% of 3–7 μm platelets; (b) sample with 5 wt% of 10–15 μm platelets.

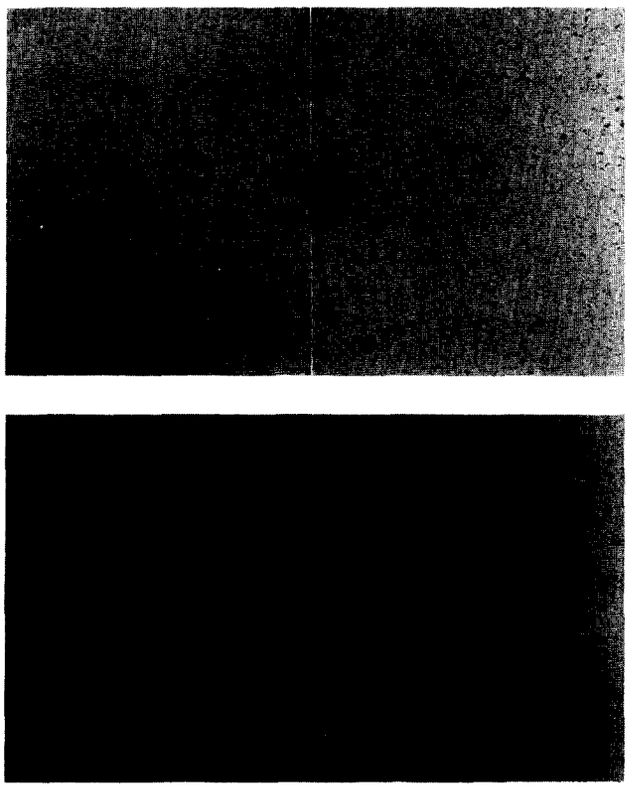

Fig. 7. Optical micrographs of Vickers indentation cracking at 200 N: (a) sample without platelets; (b) sample with 5 wt% of small platelets.

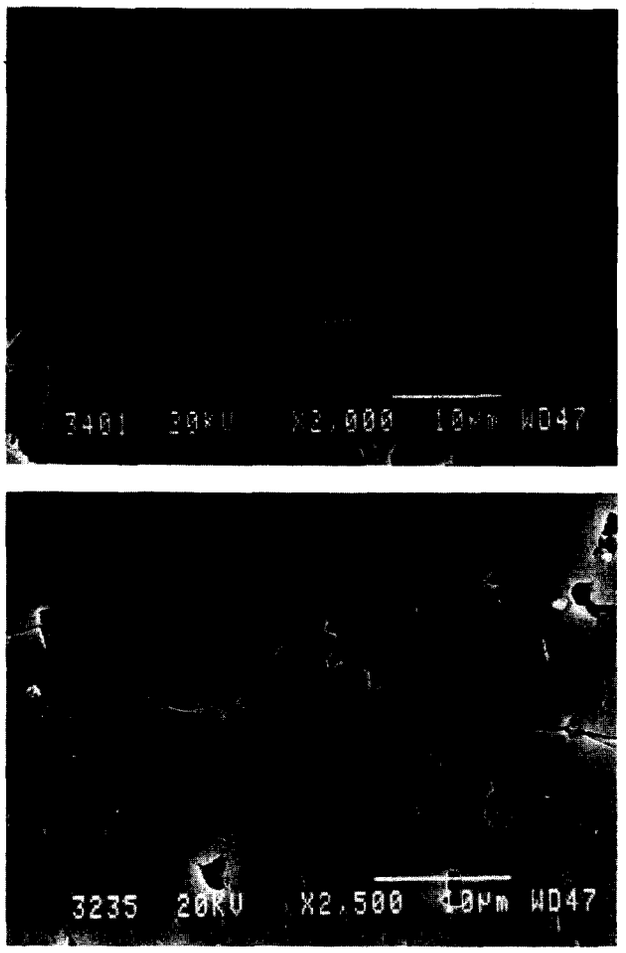

Fig. 8. SEM micrographs of Vickers indentation cracking at 200 N: (a) crack propagation parallel to the direction of original seed platelet alignment; (b) crack propagation perpendicular to the direction of original seed platelet alignment.

strain of about -5×10^{-4} and a maximum tensile strain perpendicular to the *c*-axis of about $2{\cdot}6 \times 10^{-4}$. In a *c*-axis textured alumina containing some randomly oriented material, the thermal strain in the textured material will be reduced, while that in the residual, randomly-oriented material will increase. The residual strain measurements made in the present work on a sample tile containing no seed platelets gave an average strain value for the 41·6 reflection (the only suitable high-angle, strong reflection close to the *c*-axis) of $-1{\cdot}4 \times 10^{-4}$, while that measured from the same reflection parallel and perpendicular to the *c*-axis of a strongly textured sample gave compressive strains of $-2{\cdot}4 \times 10^{-4}$ and $-0{\cdot}2 \times 10^{-4}$, respectively. The former value is associated with the strain in the small volume fraction of residual, randomly oriented grains, which are strongly constrained by the surrounding textured material, while the latter value is that associated with the dominant volume fraction of highly textured grains. The implication is that, as predicted, the textured material has a much reduced level of thermal stress.

Discussion

The present results have demonstrated a significant improvement in the mechanical properties of a textured alumina produced by gel-casting a slip containing aligned alumina seed platelets, in spite of the residual porosity and large grain size of this material. These results were obtained with high levels of calcium doping (of the order of 0·5%), due to the use of calcium as the gelling cation (the commonest cation used to promote the alginate gel reaction).

The microstructural observations on the sintered samples seeded with both sizes of alumina platelets showed that the matrix powder for the most part had been consumed during sintering to leave large, non-equiaxed, highly textured grains which had formed by the growth of the aligned seed platelets. The distribution of the seed platelets influenced both the final texture and the degree to which the grains are non-equiaxed, and the final grain size depended on both the volume fraction of the seed platelets and their initial size. The smaller platelets gave the smaller final grain size at a given loading of seed platelets and, consistent with this, the best mechanical properties. Further improvements could presumably be anticipated if the seed platelet size were to be further reduced, leading to a smaller ultimate grain size due to the greater number density of platelets at the same loading.

Calcium was selected as the gelling cation, since the calcium alginic ion-exchange reaction is well-characterized. However, calcium is known to cause abnormal grain growth which is expected to degrade the mechanical properties. Several cations have been used to gel the water-based tape used in this work[7] and satisfactory results have been achieved with alternative alumina cation dopants which are considered either beneficial (Y, Ce, La) or harmless (Sr and Ba).

The present large grain size, monolithic alumina, produced by the sintering of green bodies which contain well-aligned alumina seed platelets, is highly textured and constitutes a new class of monolithic ceramic which could have some interesting applications. These materials could be used for any wear or abrasion resistant component requiring improved crack propagation resistance normal to the surface, while the large grain size should lead to improved microstructural stability at high temperatures, and hence to improved creep resistance. The wet, gelled tape, which is produced by the gel-casting process,[7] is an intermediate product which could be wound to form tube or plastically shaped. The present results have shown that the crystalline texture reduces the thermal stresses and should also improve the thermal shock resistance, leading to potential applications as furnace tubes in electronic substrate furnaces (which are generally made only from alumina). Since only small quantities of the seed platelets are required, the increased raw material costs are minimal, while the proposed processing route is relatively uncomplicated and requires only pressureless sintering.

Conclusions

(1) A textured alumina, produced from a gel-cast slip containing aligned alumina seed platelets by tape lay-up, filter-pressing and pressureless sintering, has been found to possess good mechanical properties.
(2) Although the sintered seeded product had a far larger grain size than an equivalent, unseeded alumina, the bend strength could be enhanced by more than 20%, while the fracture toughness was unaffected.
(3) The Weibull modulus was also improved by processing with the aligned seed platelets.
(4) The Vickers hardness was only slightly reduced in the textured material, presumably due to the increased grain size.
(5) The crystalline texture and microstructural anisotropy (large, plate-like grains) inhibit crack propagation in the through-thickness direction, as demonstrated by Vickers indentation cracking.
(6) The residual thermal stresses, as determined by X-ray diffraction peak shift measurements, are significantly reduced in the textured alumina to less than one third of their value in randomly oriented alumina samples subjected to the same sintering cycle.
(7) The texture (preferred orientation) and the microstructural anisotropy (non-equiaxed grain structure) are both associated with the growth of the aligned seed platelets into the fine-grained matrix during the pressureless sintering process.

Acknowledgements

The authors would like to acknowledge the provision of research funding for this project by Elf-Atochem, as well as the encouragement and support of Dominique Cotto and Jacques Macé, of Elf-Atochem. We would also like to acknowledge the support of the French government for one of us (T.C.) under their VSN programme.

References

1. Farkash, M. & Brandon, D., Whisker alignment by slip extrusion. *Mater. Sci. Engng. A*, **177** (1994) 269–75.
2. Baril, D., Tremblay, S. P. & Fiset, M., Silicon carbide platelet-reinforced silicon nitride composites. *J. Mater. Sci.*, **28** (1993) 5486–94.
3. Poorteman, M., Descamps, P., Cambier, F., Leriche, A. & Thierry, B., Hot isostatic pressing of SiC-platelets/Y-TZP composites. *J. Eur. Ceram. Soc.*, **12** (1993) 103–9.
4. Poorteman, M., Descamps, P. & Cambier, F., Superplastic deformation of alumina platelets reinforced Y-TZP. *3rd. Euro-Ceramics*, ed. P. Duràn and J. F. Fernàndez. Faenza Editrice Ibérica S. L., 1993, Vol. 3, pp. 659–64.
5. Faber, K. T. & Evans, A. G., Crack deflection processes — I. Theory. *Acta Metall.* **31**(4) (1983) 565–76.
6. Faber, K. T. & Evans, A. G., Crack deflection processes — II. Experiment. *Acta Metall.*, **31**(4) (1983) 577–84.
7. Carisey, T., Laugier-Werth, A. & Brandon, D. G., Control of texture in Al_2O_3 by gel-casting. *J. Eur. Ceram. Soc.*, **15** (1995) 1–8.
8. Quinn, G. D., Baratta, F. I. & Conway, J. A., Commentary on U.S. Army standard test method for flexural strength of high performance ceramics at ambient temperature. Army Materials and Mechanics Research Center. (08-1985). AMMRC 85–21.
9. Fantozzi, G., Rupture des matériaux 1ère et 2 ième parties. Departement Génie Physique des Matériaux. INSA Lyon édition. (1992).
10. Creyke, W. E. C., Sainsbury, I. E. J. & Morrell, R., *Design with Non-ductile Materials*. Appl. Sci. Publ., 1982.
11. Henshall, J. L., Rowcliffe, D. J. & Edington, J. E. W., Fracture parameters in Refel silicon carbide. *J. Mater. Sci.*, **9** (1974) 1559–61.
12. Srinivasan, M. & Seshadri, S. G., Application of single edge notched beam and indentation techniques to determine fracture toughness of alpha silicon carbide. *Fracture Mechanics Methods for Ceramics, Rocks, and Concrete*, Am. Soc. Test. Matls. STP 745, ed. S. W. Freiman and E. R. Fuller, Jr. ASTM, Philadelphia, PA, 1981, pp. 46–86.
13. Levin, I., Kaplan, W. D. & Brandon, D. G., Residual stresses in alumina-SiC nanocomposites. *Acta Metal. et Mater.*, **42**, (1994) 1147.